**Ilie Talpasanu**
Department of Electronics and Mechanical,
Wentworth Institute of Technology,
550 Huntington Ave,
Boston, MA 02115-5998
e-mail: talpasanui@wit.edu

**T. C. Yih**
Vice Provost for Research,
Oakland University,
2200 N. Squirrel Road,
Rochester, MI 48309–4401
e-mail: vih@oakland.edu

**P. A. Simionescu**
Department of Mechanical Engineering,
The University of Tulsa,
600 South College Ave,
Tulsa, OK 74104-3989
e-mail: psimionescu@utulsa.edu

# Application of Matroid Method in Kinematic Analysis of Parallel Axes Epicyclic Gear Trains

*A novel method for kinematic analysis of parallel-axes epicyclic gear trains is presented, called the incidence and transfer method, which uses the incidence matrices associated with the edge-oriented graph associated to the mechanism and the transfer joints (teeth contact joints). Relative to such joints, a set of independent equations can be generated for calculating the angular positions, velocities, and accelerations. Complete kinematic equations are obtained in matrix form using a base of circuits from a cycle matroid. The analysis uses the relationships between the number of mobile links, number of joints, and number of circuits in the base of circuits, together with the Latin matrix (whose entries are function of the absolute values of the partial gear ratios of the transmission). Calculating the rank of the Latin matrix can identify singularities, like groups of gears that rotate as a whole. Relationships between the output and input angular velocities and accelerations are then determined in a matrix-based approach without using any derivative operations. The proposed method has general applicability and can be employed for systems with any number of gears and degrees of freedom, as illustrated by the numerical examples presented.* [DOI: 10.1115/1.2337310]

## 1 Introduction

The most commonly used method for kinematic analysis of parallel axes epicyclic gear trains (EGTs) is the Willis method of motion inversion [1]. Analytic methods of generating the kinematic equations of EGTs based on the relative motions within the mechanism are also available [2–5], as well as graphical methods [2,5]. The latter are difficult to implement in computer algorithms, being however useful to check the results obtained using other analytical methods. The above methods lack generality, and can become cumbersome in case of gear trains with a large number of gears and multiple degrees of freedom. Tabular methods [6–8] developed based on Willis' inversion method are somehow easier to apply but they cannot be extended to transmissions with non-parallel axes. In recent years, new methods have been developed using the graph associated with the mechanism and the fundamental circuit concept [9–14]. In case of non-oriented graphs, the fundamental circuits required to generate the kinematic equations of the EGTs can be identified using the adjacency matrix [15] and incidence matrix method [16,17]. The generation of the adjacency matrix of the non-oriented graphs associated with the mechanism requires either defining some general rules [15] or using a modulo 2 approach [16], while the use of incidence matrices is a straightforward, easy to apply method [17]. Algorithms based on these methods were developed for transmission error computation [16], which can lead to unfavorable behavior of the real transmission [18,19]. In an earlier paper by the first author [20], oriented-graph and the incidence-matrix methods were also used in the design and analysis of planar and spatial mechanisms.

Matroid Theory (which combines the properties of graphs and matrices) appears to be less known to the mechanism community. Matroids were used to define the rigidity of trusses [21,22] and in the study of electrical and mechanical systems [23]. An efficient kinematic and dynamic analysis of mechanical systems using a base of circuits from a cycle matroid was developed in [24].

In this paper a systematic approach for the generation the kinematic equations of any EGT, that is suited to computer implementation and automatic generation of the respective equations, is proposed.

Contributed by the Power Transmission and Gearing Committee of ASME for publication in the JOURNAL OF MECHANICAL DESIGN. Manuscript received May 24, 2005; final manuscript received January 23, 2006. Review conducted by Teik C. Lim. Paper presented at the ASME 2005 Design Engineering Technical Conferences and Computers and Information in Engineering Conference (DETC2005), September 24, 2005–September 28, 2005, Long Beach, CA.

## 2 Oriented Graphs Attached to Kinematic Chains

**2.1 Link and Joint Numbering.** For the case of an epicyclic transmission with $n$ mobile links and $k$ joints, link numbering begins with 0 assigned to the ground element (casing) continuing up to $n$ for the other mobile links. Additionally, the turning joints and meshing joints (also called transfer joints) are assigned numbers between $n+1$ and $n+k-c$ and between $n+k-c+1$ and $n+k$ respectively.

Figure 1(*a*) shows the numbering in a typical EGT mechanism with $n=4$ mobile links: 1 (sun gear), 2 (ring gear), 3 (carrier), and 4 (planet gear). There are $k=6$ joints (5, 6, 7, 8, 9, 10), with $k-c=4$ turning joints (5, 6, 7, 8) and $c=2$ meshing (transfer) joints (9, 10).

**2.2 EGT Associated Graph.** A graph $G=(V,E)$ is defined as a collection of $m=n+1$ vertices $V=\{v_0,v_1,\ldots,v_n\}$ connected by a set of $k$ edges $E=\{e_1,e_2,\ldots,e_k\}$ [25]. A *path* is defined as a sequence $[v_0,e_1,v_1,e_2,\ldots,v_n]$, with all vertices $v_0$ to $v_n$ different. A path with $v_0=v_n$ is a *circuit* (*cycle*). In a connected graph $G$, by cutting one by one the $c$ edges contained in its circuits, a *spanning tree* of the graph (further noted $B$) is obtained [26]. A spanning tree contains the same number of vertices $m$ as the graph and has $m-1=n$ edges. The set of $c$ cut edges is called a *complement set* $E(G)$–$E(B)$ and will be further represented as dashed lines inside the graph. If $e$ is one of the edges from the complement set, then $B\cup\{e\}$ contains one circuit. Repeating this procedure for all edges of the complement set, one could get $c$ *independent circuits*. For a graph $G$ Euler's formula [21] holds:

$$c=k-n \tag{1}$$

For the sample mechanism in Fig. 1(*a*), Fig. 1(*b*) shows its associated graph. This graph has $m=5$ vertices: $V(G)=\{0,1,2,3,4\}$ and $k=6$ edges: $E(G)=\{5,6,7,8,9,10\}$. The spanning tree has $m=5$ vertices: $V(B_1)=V(G)=\{0,1,2,3,4\}$, and $n=4$ edges: $E(B_1)=\{5,6,7,8\}$.

The complement set of cut edges shown in dashed line is:

  

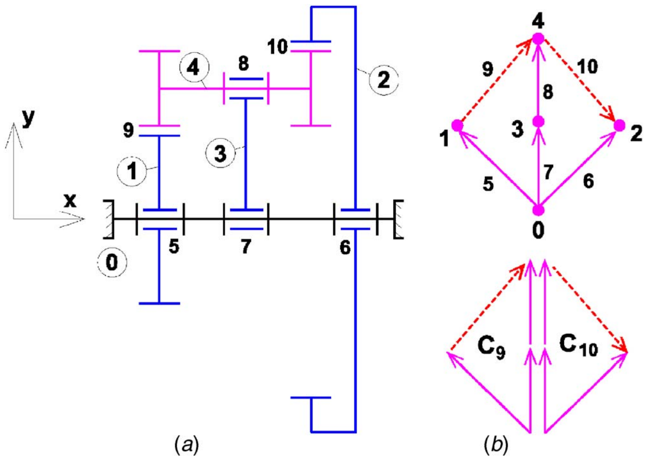

**Fig. 1 (a) EGT mechanism and (b) graph and circuits**

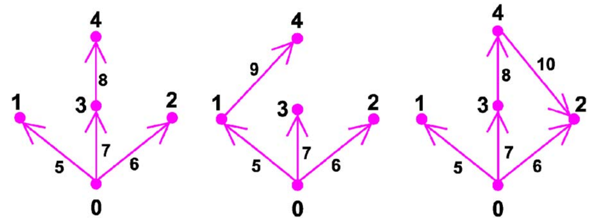

**Fig. 2 Spanning trees for the graph**

$E(G)$–$E(B_1)$=$\{9,10\}$, and contains $c$=2 edges corresponding to the transfer joints (meshing joints) of the mechanism. The set $c=k-n$=2 *independent circuits* is $\{C_9, C_{10}\}$ and is obtained adding one by one the edges from the complement set to the spanning tree, as follows: adding edges labeled 9 and 10, the circuits $C_9=\{5,7,8,9\}$, and $C_{10}$=$\{6,7,8,10\}$ are obtained. This set $\{C_9, C_{10}\}$ will be further called a *base of independent circuits*.

**2.3 Graph Edges Orientation.** An oriented-edge graph is called a *digraph*. To each edge $e$, a pair of numbers $(v^-, v^+)$ is assigned according to the desired input/output parameters, and the edge is represented as an arrow oriented from vertex $v^-$ to vertex $v^+$. For example, if joint $e$ (edge graph) connects links 1 to the fixed link 0, then the pair $(v^-, v^+)=(0,1)$ will be assigned to it. For the oriented graph in Fig. 1(*b*) the following node-edge connections exist:

$$5 \to (0,1), 6 \to (0,2), 7 \to (0,3), 8 \to (3,4), 9 \to (1,4), 10 \to (4,2).$$

## 3 Matrix Description of the Oriented Graph

**3.1 Incidence Vertex-Edge Matrix $^0\Gamma$.** Various matrix representations of graphs have been proposed, the most commonly being the *incidence vertex-edge matrix*. This $(m \times k)$ matrix $^0\Gamma$ has its entries $g_{m,k}$ equal to $-1$ if $v=v^-$, equal to $+1$ if $v=v^+$, and equal to 0 for all other vertices. Consequently, each column $k$ will have $a$ $-1$ and $a$ $+1$ entry corresponding to the two vertices connected by the respective edge. For the oriented graph in Fig. 1(*b*), the incidence matrix will therefore be:

$$\begin{array}{c} \\ \\ {}^0\Gamma = \end{array}\begin{array}{c|c} & \begin{array}{cccccc} 5 & 6 & 7 & 8 & 9 & 10 \end{array} \\ \begin{array}{c} 0 \\ 1 \\ 2 \\ 3 \\ 4 \end{array} & \left[\begin{array}{cccc|cc} -1 & -1 & -1 & 0 & 0 & 0 \\ \hline 1 & 0 & 0 & 0 & -1 & 0 \\ 0 & 1 & 0 & 0 & 0 & 1 \\ 0 & 0 & 1 & -1 & 0 & 0 \\ 0 & 0 & 0 & 1 & 1 & -1 \end{array}\right] \end{array} \qquad (2)$$

**3.2 Reduced Incidence Vertex-Edge Matrix.** This $(n \times k)$ matrix $\Gamma$ is obtained by deleting from the incidence vertex-edge matrix the first row corresponding to the fixed link. Euler's formula, $k=n+c$, also holds for the graph attached to the epicyclic transmission mechanism with $n$ mobile links (vertices graph), $k$ joints (edges graph), and $c$ independent circuits. As a consequence, the reduced-incidence matrix is partitioned in two submatrices: a $(n \times n)$ matrix $G$, with the number of columns equal to the number of turning joints (edges of the spanning tree), and a $(n \times c)$ matrix $^*G$, with the number of columns equal to the number of meshing joints (transfer-complement edges) of the mechanism. For the oriented graph in Fig. 1(*b*), the reduced incidence matrix will therefore be:

$$\Gamma = [G_{n,n} | {}^*G_{n,c}] = \begin{array}{c|c} & \begin{array}{cccccc} 5 & 6 & 7 & 8 & 9 & 10 \end{array} \\ \begin{array}{c} 1 \\ 2 \\ 3 \\ 4 \end{array} & \left[\begin{array}{cccc|cc} 1 & 0 & 0 & 0 & -1 & 0 \\ 0 & 1 & 0 & 0 & 0 & 1 \\ 0 & 0 & 1 & -1 & 0 & 0 \\ 0 & 0 & 0 & 1 & 1 & -1 \end{array}\right] \end{array} \qquad (3)$$

**3.3 Path Matrix of the Oriented Graph.** This $(n \times n)$ matrix $Z$ constructed from the spanning tree has its entries $z_{n,k}$ defined as follows: $z_{n,k}$=−1 if edge $k$ belongs to the path from vertex 0 (ground) to vertex $n$ and is oriented away from vertex 0; $z_{n,k}$= +1 if edge $k$ belongs to the path from the vertex 0 to vertex $n$ and is oriented toward vertex 0, and $z_{n,k}$=0 if edge $k$ does not belong on the path.

For the mechanism in Figs. 1(*a*) and three of the spanning trees are shown in Fig. 2; the path matrix for tree (*a*) in Fig. 2(*a*) being:

$$Z = \begin{array}{c|c} & \begin{array}{cccc} 1 & 2 & 3 & 4 \end{array} \\ \begin{array}{c} 5 \\ 60 \\ 7 \\ 8 \end{array} & \left[\begin{array}{cccc} -1 & 0 & 0 & 0 \\ -1 & 0 & 0 & \\ 0 & 0 & -1 & -1 \\ 0 & 0 & 0 & -1 \end{array}\right] \end{array} \qquad (4)$$

One can check that the following relations, important to the kinematic analysis of the mechanism, hold:

$$ZG = GZ = -U \quad \text{and} \quad Z^TG^T = G^TZ^T = -U \qquad (5)$$

where $U$ is the $(n \times n)$ unit matrix.

**3.4 Spanning-Tree Matrix.** This $(c \times n)$ matrix $B$ is defined based on the incidence matrices $Z$ and $^*G$ as follows:

$$B = {}^*G^TZ^T \qquad (6)$$

where the superscript $T$ designates the transpose operation.

**3.5 Independent Circuit-Edge Incidence Matrix.** This $(c \times k)$ matrix $I$ has $c$ rows equal to the number of independent circuits and $k$ columns corresponding to the edges of the graph. Since $k=n+c$, the matrix $I$ is partitioned in two submatrices: a $(c \times n)$ matrix $B$, with the number of columns equal to number of turning joints (edges of spanning tree) and a $(c \times c)$ unit matrix $^*U$ with the number of columns equal to the number of meshing joints (transfer-complement edges):

$$I = [B_{c,n} | {}^*U_{c,c}] \qquad (7)$$

An $i_{c,k}$ entry could be either equal to −1, +1, or 0 as follows. A −1 entry denotes the column label of the edge belonging to the circuit and oriented in opposite direction to the path (clockwise or counterclockwise according to the orientation of the edge cut). $A+1$ entry denotes the column label of the edge belonging to the circuit and having the same direction as the path. A 0 entry indicates that the respective edge does not belong to the circuit. The graph in Fig. 1(*b*) has as a set of two independent circuits (the two rows of

I), both in clockwise direction. Therefore, its circuit-edge independent matrix $I$ will be:

$$I = \begin{array}{c} \\ C_9 \\ C_{10}0 \end{array}\!\!\begin{array}{c} \begin{array}{cccccc} 5 & 6 & 7 & 8 & 9 & 10 \end{array} \\ \left[\begin{array}{cccc:cc} 1 & 0 & -1 & -1 & 1 & 0 \\ -1 & 1 & 1 & 0 & 1 & \end{array}\right] \end{array} \tag{8}$$

**3.6 Cycle Matroid Fundamentals.** Matroids are generalizations of graphs and matrices [27]. Let $\Gamma$ be a $(n \times k)$ matrix with $E$ being the set of column labels, and $I$ being a collection of subsets of $E$ for which the set of columns labeled by $I$ is linearly independent. The set $E$ and the members of $I$ are the *underlying* set and the *independent* sets. According to [21,25,28], the set $I$ satisfies the conditions:

1. $I$ is nonempty;
2. every subset of every member of $I$ is also in $I$ (hereditary condition); and
3. if $X$ and $Y$ are in $I$ and $|X| = |Y| + 1$, then there is an element $x$ in $X - Y$ such that $Y \cup \{x\}$ is in $I$ (augmentation condition).

Consider a graph $G = (V, E)$, where $E$ is the edge set, $V$ is the vertex set. Let $I$ be the set of subsets of $E$ that do not contain all of the edges of any cycle of $G$. The pair $M[G] = (E, I)$ is called a *cycle matroid*. The *bases* are the sets of edges of a spanning tree of $G$, and are maximally independent sets: $\{B \subseteq E \mid B$ is the set of a spanning tree of $G\}$. The *circuits* are the sets of edges which form cycles in $G$, and are minimally dependent sets: $\{C \subseteq E \mid C$ is the set of edges of a simple cycle of $G\}$. The cycle matroid $M[G]$ is defined also in terms of its circuits. Based on properties 1–3 above, it was shown that for the collection $C$ of circuits of a matroid the following properties hold [27]:

4. the empty set is not in $C$;
5. no member is a proper subset of another member of $C$; and
6. if $C_1$ and $C_2$ are members of $C$ and $e \in C_1 \cap C_2$, then $(C_1 \cup C_2) - \{e\}$ contains a member of $C$.

The *bases* are maximum independent sets of cycles, and their independency is evidenced by the independent rows in the incidence circuit edges matrix.

*Example*. For the graph in Fig. 1($b$), the set $E$ of column labels is $\{5,6,7,8,9,10\}$. Some sets of maximal linear independent columns (bases) in matrix $\Gamma$, Eq. (3) are: $B_1 = \{5,6,7,8\}$, $B_2 = \{5,6,7,9\}$, and $B_3 = \{5,6,7,10\}$. The edges labeled by the bases correspond to the spanning trees, as shown in Fig. 2. A collection of minimally dependent sets of columns (circuits) in matrix $\Gamma$ are: $C_9 = \{5,7,8,9\}$, $C_{10} = \{6,7,8,10\}$, and $C_{9+10} = \{5,6,9,10\}$. The bases of circuits are maximum independent sets of cycles: $\{C_9, C_{10}\}$, $\{C_9, C_{9+10}\}$, $\{C_{10}, C_{9+10}\}$ and they also describe the cycle matroid. Notice that the set $\{C_9, C_{10}, C_{9+10}\}$ is not included because is not an independent set. From the incidence circuit edges matrix $C$:

$$C = \begin{array}{c} \\ C_9 \\ C_{10} \\ C_{9+10} \end{array}\!\!\begin{array}{c} \begin{array}{cccccc} 5 & 6 & 7 & 8 & 9 & 10 \end{array} \\ \left[\begin{array}{cccccc} 1 & 0 & -1 & -1 & 1 & 0 \\ 0 & -1 & 1 & 1 & 0 & 1 \\ 1 & -1 & 0 & 0 & 1 & 1 \end{array}\right] \end{array} \tag{9}$$

It can be seen that the entries on the third row can be obtained by adding the first and the second row, therefore the set $\{C_9, C_{10}, C_{9+10}\}$ is dependent. Fig. 2($a$) shows the spanning tree for the base of independent circuits $\{C_9, C_{10}\}$ the circuit-edge independent matrix of which was computed with Eq. (8). Fig. 2($b$) and 2($c$) show the other two spanning trees corresponding to the bases of independent circuits $\{C_9, C_{9+10}\}$, and $\{C_{10}, C_{9+10}\}$. The following first important rule applies:

RULE 1. *The kinematic analysis developed on each of the bases of independent circuits in the cycle matroid leads to the same result, which means that it is sufficient to be performed on only one of the bases of independent circuits.*

**3.7 Joint-Position Matrix.** This $(c \times k)$ matrix $Y$ has its entries defined as the product $i_{c,k} \cdot y_{k,k}$, where $y_k$ and $y_{*k}$ are the $y$ coordinates of joint $k$ and complement edge $^*k$, respectively. The term $i_{c,k}$ is the entry from the incidence matrix $I$ and $y_{*k,k}$ is defined as: $y_{*k,k} = y_k - y_{*k}$. Matrix $Y$ can be partitioned into two submatrices: a $(c \times n)$ matrix $R$, and a $(c \times c)$ matrix $^*O$ with zero entries. For the graph in Fig. 1($b$), this partitioning is:

$$Y = \left[\begin{array}{cccc:cc} y_{9,5} & 0 & y_{9,7} & -y_{9,8} & y_{9,9} & 0 \\ 0 & -y_{10,6} & y_{10,7} & y_{10,8} & 0 & y_{10,10} \end{array}\right] = [\mathbf{R}_{c,n} \,\vdots\, {}^*O_{c,c}] \tag{10}$$

It is to be noticed that submatrix $R$ above is a function of the pitch diameters $d_1$, $d_2$, $d'_4$, $d''_4$ of the sun, ring, and of the two wheels in the compound planet 4 as follows:

$$\begin{bmatrix} y_{9,5} & 0 & y_{9,7} & -y_{9,8} \\ 0 & -y_{10,6} & y_{10,7} & y_{10,8} \end{bmatrix} = \begin{bmatrix} -d_1/2 & 0 & d_1/2 & -d'_4/2 \\ 0 & d_2/2 & -d_2/2 & -d''_4/2 \end{bmatrix} \tag{11}$$

**3.8 Latin Matrix.** This is a $(c \times n)$ matrix $\mathbf{\Lambda}$ whose entries are computed with the following relation:

$$\mathbf{\Lambda} = RG^T \tag{12}$$

The Latin matrix is important to the kinematic analysis in that its entries are the coefficients of the velocity equations. If the equation $n = E + c$ (that will be derived in the next paragraph) is applied to a mechanism with $E$ degrees of freedom and $c$ cycles, then the Latin matrix is partitioned into two submatrices: a $(c \times E)$ matrix $L$, and a $(c \times c)$ matrix $^0L$ as follows:

$$\Lambda = [L_{c,E} \,\vdots\, {}^0L_{c,c}] \tag{13}$$

Similarly to matrix $R$, the entries of the Latin matrix $\mathbf{\Lambda}$ are functions of the pitch diameters of the wheels, as shown in Eq. (14) for the actual case of the mechanism in Fig. 1($b$):

$$\begin{bmatrix} y_{9,5} & 0 & y_{7,8} & y_{8,9} \\ 0 & y_{6,10} & y_{8,7} & y_{10,8} \end{bmatrix} = \begin{bmatrix} -d_1/2 & 0 & (d_1 + d'_4)/2 & -d'_4/2 \\ 0 & d_2/2 & (d''_4 - d_2)/2 & -d''_4/2 \end{bmatrix} \tag{14}$$

**Relation Between Number of Joints, Links, Fundamental Circuits and Degrees of Freedom.** When all constraints of a planar EPG mechanism with $n$ moving links are suspended, there will be a total of $3n$ mobilities. The turning joints $k_r$ in the mechanism, each allowing only one mobility, will reduce these $3n$ mobilities by $2k_r$. In turn, meshing joints $k_c$, each with a mobility of two, will further reduce this number by $k_c$. Thus the Kutzbach criterion [29] for the total number of degrees of freedom of the mechanism becomes:

$$E = 3n - 2k_r - k_c \tag{15}$$

Since for the case of gear trains the number of mobile links equals the number of turning joints $k_r = n$, the total number of joints will therefore be $k = k_r + k_c = n + k_c$. By equating $k$ from Euler's equation for the associated graph: $k = n + c$, one can conclude that $k_c = c$ (i.e., the number of meshing joints equals the number of independent circuits) a conclusion also reached by Tsai [12] in a different approach. With these findings the above relation (15) simplifies to:

$$E = n - c \tag{16}$$

**Table 1 Velocity ratios and determinants of Matrix $^0L$**

| | $e^c_{s,r}$ | $e^s_{c,r}$ | $e^r_{s,c}$ | $e^s_{r,c}$ | $e^c_{r,s}$ | $e^r_{c,s}$ |
|---|---|---|---|---|---|---|
| Velocity ratio | $\frac{e}{1}$ | $\frac{1-e}{1}$ | $\frac{e}{e-1}$ | $\frac{1}{1-e}$ | $\frac{1}{e}$ | $\frac{e-1}{e}$ |
| Determinant | 1 | 1 | $e-1$ | $e-1$ | $-e$ | $-e$ |

## 4 Velocity Analysis for Gear Trains With Parallel Axes of Rotation

**4.1 Absolute Angular Velocity Matrix.** $\omega$ is a $(n\times 1)$ column vector. Its entries are the absolute velocities (velocities relative to the fixed frame) assigned to all vertices, i.e., the links of the mechanism (gears and gear carriers). In order to have determinate motion, for an EGT mechanism with $E$ degrees of freedom, $E$ independent absolute velocities must be known. Since $n=E+c$, then the $\omega$ column matrix can be partitioned into one known (input) $\boldsymbol{\omega_E}$ of dimension $E$ and one unknown (output) vector $\omega_c$ of dimension $c$, respectively:

$$\omega=(\omega_E \mid \omega_c)^T \tag{17}$$

For the actual case of the mechanism in Fig. 1, the velocity matrix is:

$$\omega=(\omega_1 \quad \omega_2 \quad \omega_3 \quad \omega_4)^T \tag{18}$$

**4.2 Absolute Angular Velocity Equation.** As will be shown later, the absolute angular velocities of the mobile links are given by:

$$\Lambda\cdot\omega=0_c \tag{19}$$

with $0_c$ the $(c\times 1)$ zero column vector. For each meshing joint $k_c$ the *tooth ratio* $i_k$ is defined as a positive number $i_k=N_t/N_h=d_t/d_h$, where $N_t$ is the number of teeth of the input gear (the tail vertex in the graph), $N_h$ is the number of teeth of the output gear (the head vertex in the graph); $d_t$ and $d_h$ are the pitch diameters of the respective gears.

Dividing each row by the respective pitch diameter, the Latin matrix $\boldsymbol{\Lambda}$ is transformed and becomes function of the teeth numbers.

For the graph in Fig. 1($b$), the teeth ratios are $i_9=N_1/N_4'=d_1/d_4'$ and $i_{10}=N_4''/N_2=d_4''/d_2$.

Dividing the first row in the corresponding Eq. (19) by $d_4'$ and the second row by $d_2$ the following new form is obtained:

$$\begin{bmatrix}-i_9 & 0 & i_9+1 & -1\\ 0 & 1 & i_{10}-1 & -i_{10}\end{bmatrix}\cdot\begin{pmatrix}\omega_1\\ \vdots\\ \omega_4\end{pmatrix}=\begin{pmatrix}0\\0\end{pmatrix} \tag{20}$$

**4.3 Solution of the Angular Velocity Equation.** In Eq. (19) there are $E$ known input angular velocities and a number of $n-E=c$ unknown angular velocities (equal to the number of equations). Therefore the solution of Eq. (19) will be of the form:

$$(\omega_c)=-[^0L]^{-1}[L_{c,E}](\omega_E) \tag{21}$$

For the mechanism in Fig. 1($a$), and for all possible input/output combinations, Equation (21) yields the following four possible solutions:

$$(1)\ \text{Input: } \omega_E=(\omega_1 \quad \omega_3)^T\cdot \text{Output:} \omega_c=\begin{pmatrix}\omega_2\\ \omega_4\end{pmatrix}$$
$$=\begin{pmatrix}-i_9i_{10}\omega_1+(i_9i_{10}+1)\omega_3\\ -i_9\omega_1+(i_9+1)\omega_3\end{pmatrix} \tag{22}$$

$$(2)\ \text{Input: } \omega_E=(\omega_1 \quad \omega_2)^T\cdot \text{Output: } \omega_c=\begin{pmatrix}\omega_3\\ \omega_4\end{pmatrix}$$
$$=\begin{pmatrix}i_9i_{10}/(i_9i_{10}+1)\omega_1+1/(i_9i_{10}+1)\omega_2\\ (i_9i_{10}-i_9)/(i_9i_{10}+1)\omega_1+(i_9+1)/(i_9i_{10}+1)\omega_2\end{pmatrix} \tag{23}$$

$$(3)\ \text{Input: } \omega_E=(\omega_2 \quad \omega_3)^T \text{ Output: } \omega_c=\begin{pmatrix}\omega_1\\ \omega_4\end{pmatrix}$$
$$\times\begin{pmatrix}-1/i_9i_{10}\omega_2+(i_9i_{10}+1)/i_9i_{10}\omega_3\\ 1/i_{10}\omega_2+(i_{10}-1)/i_{10}\omega_3\end{pmatrix} \tag{24}$$

$$(4)\ \text{Input: } \omega_E=(\omega_3 \quad \omega_4)^T\cdot \text{ Output: } \omega_c=\begin{pmatrix}\omega_1\\ \omega_2\end{pmatrix}$$
$$=\begin{pmatrix}(1+1/i_9)\omega_3-1/i_9\omega_4\\ (1-i_{10})\omega_3+i_{10}\omega_4\end{pmatrix} \tag{25}$$

It is to be noticed that when solving the above set of Eqs. (20) in the unknowns $i_9$ and $i_{10}$, Willis form of the kinematic equations for each circuit is obtained:

$$i_9=-\frac{\omega_4-\omega_3}{\omega_1-\omega_3} \quad \text{and} \quad i_{10}=+\frac{\omega_2-\omega_3}{\omega_4-\omega_3} \tag{26}$$

The minus sign in front of the first fraction shows that the relative rotations $\omega_{3,4}$, $\omega_{3,1}$ are opposite while the plus sign in front of the second equation shows that $\omega_{3,2}$ and $\omega_{3,4}$ are in the same direction.

The *velocity ratio*, defined as the ratio of the output to input angular velocities [30], and noted $e^f_{i,o}$ ($i$, $o$, and $f$ stand for input, output, and fixed link, respectively), can also be calculated and has been gathered in Table 1. One can conclude that the determinants of $^0L$ matrices are the denominators in the velocity ratios, and for any negative value $e=-i_9\cdot i_{10}$, there are four positive and two negative values of the velocity ratios.

**4.4 Potential Group of Wheels Rotating as a Whole.** These are wheels that have the same absolute angular velocity. The system of Eq. (19) can be written in the following form:

$$[L_{c,E} \mid {}^0L_{c,c}]\begin{pmatrix}\omega_E\\ ---\\ \omega_c\end{pmatrix}=(0_c) \tag{27}$$

and the equivalent system is obtained

$$[\lambda \mid {}^0L_{c,c}]\begin{pmatrix}1\\ ---\\ \omega_c\end{pmatrix}=(0_c) \tag{28}$$

where the $(c\times 1)$ column matrix $\lambda$ is obtained by multiplying the $(c\times E)$ matrix $L$ with the known (input) matrix $\omega_E$

$$(\lambda)=\begin{pmatrix}\lambda_1\\ \vdots\\ \lambda_c\end{pmatrix}=[L_{c,E}](\omega_E) \tag{29}$$

By applying Cramer rule to the system (28), the following solution is obtained:

$$\frac{1}{\Delta}=\frac{\omega_{E+1}}{(-1)^{2E+1}\Delta_{E+1}}=\frac{\omega_{E+2}}{(-1)^{2E+2}\Delta_{E+2}}=\cdots=\frac{\omega_{E+c}}{(-1)^{2E+c}\Delta_{E+c}} \tag{30}$$

The determinant $\Delta=\det[^0L]$ is obtained removing the first column in matrix $[\lambda \mid {}^0L]$, while the determinants: $\Delta_{E+1}$, $\Delta_{E+2}$, $\Delta_{E+c}$ are obtained by removing one by one the next $c$ columns.

If two or more wheels have the same scalar angular velocities (i.e., same values for the numerators labeled in the above equations), then the determinants (denominators) labeled with the same numbers should also be equal.

Based on the analysis of the circuits, a method to detect degenerate structures in planetary gear trains was also developed in [31].

**4.5 Relative Angular Velocity Matrix.** $\hat{\omega}$ is a $(k\times 1)$ column matrix of entries $\hat{\omega}_k=\omega_{t,h}=+\omega_h-\omega_t$ i.e. the relative angular velocities assigned to all edges (joints) as the difference of absolute velocities. The pair of numbers +1 and −1 is the same as in the columns of matrix Γ. Since $k=n+c$, the matrix $\hat{\omega}$ is partitioned into two submatrices: a $(n\times 1)$ column matrix $\hat{\omega}_n$ whose entries are the $n$ relative velocities in the turning joints (edges of the spanning tree), and a $(c\times 1)$ matrix ${}^*\hat{\omega}_c$ with $c$relative velocities in the meshing joints (complement set edges)

$$\hat{\omega}=(\hat{\omega}_n \mid {}^*\hat{\omega}_c)^T \tag{31}$$

For the graph in Fig. 1($b$), the column matrix of the relative angular velocities has the following form:

$$\begin{aligned}&\left(\hat{\omega}_5 \quad \hat{\omega}_6 \quad \hat{\omega}_7 \quad \hat{\omega}_8 \mid \hat{\omega}_9 \quad \hat{\omega}_{10}\right)^T\\ &\quad=\left(\hat{\omega}_{0,1} \quad \omega_{0,2} \quad \omega_{0,3} \quad \omega_{3,4} \mid \omega_{1,4} \quad \omega_{4,2}\right)^T\end{aligned} \tag{32}$$

**4.6 Equation for Relative Angular Velocities.** The relative velocities $\hat{\omega}$ of the joints can be calculated based on the values of the absolute velocities $\omega$ of the mobile links with:

$$(\hat{\omega})=\begin{bmatrix} G^T \\ --- \\ {}^*G^T \end{bmatrix}(\omega) \tag{33}$$

For the mechanism in Fig. 1($a$), with the input $\omega_E=(\omega_1\omega_3)^T$ and output $\omega_c=(\omega_2\omega_4)^T$ Eq. (22) yields:

$$\begin{pmatrix} \hat{\omega}_5 \\ \hat{\omega}_6 \\ \hat{\omega}_7 \\ --- \\ \hat{\omega}_8 \\ \hat{\omega}_9 \\ \hat{\omega}_{10} \end{pmatrix}=\begin{pmatrix} \omega_1 \\ -i_9 i_{10}\omega_1+(i_9 i_{10}+1)\omega_3 \\ \omega_3 \\ -i_9\omega_1+i_9\omega_3 \\ -(i_9+1)\omega_1+(i_9+1)\omega_3 \\ ---------------- \\ (i_9-i_9 i_{10})\omega_1+(i_9 i_{10}-i_9)\omega_3 \end{pmatrix} \tag{34}$$

**4.7 Orthogonallity Condition for Relative Angular Velocities.** The following equation holds from the multiplication of matrices I and $\hat{\omega}$:

$$\mathrm{I}\hat{\omega}=0_c \tag{35}$$

where $0_c$ is a $(c\times 1)$ column matrix with zero entries

Equation (35) represents the orthogonallity condition for relative velocities: *for every independent cycle the sum of relative angular velocities of the edges of the cycle is zero.*It is obvious that when summating relative velocities $\hat{\omega}_k=+\omega_h-\omega_t$, each absolute angular velocity $\omega_h$ and $\omega_t$ will show twice and have opposite sign, therefore satisfying the above condition (35).

Based on Eqs. (7) and (35), the following relation between the angular velocities of the $c$ meshing joints and the $n$ velocities of the revolute joints can be obtained:

$$\hat{\omega}_c=B\,\hat{\omega}_n \tag{36}$$

This equation allows the set of $c$ unknown relative angular velocities $\hat{\omega}_c$ to be calculated.

For the example mechanism in Fig. 1($a$), the two sets of parallel vectors have their resultant scalars: $\hat{\omega}_9=\hat{\omega}_5-\hat{\omega}_7-\hat{\omega}_8$ for the first cycle and $\hat{\omega}_{10}=-\hat{\omega}_6+\hat{\omega}_7+\hat{\omega}_8$ for the second cycle. Considering the moment of each set of parallel vectors relative to the transfer (meshing) joints 9 and 10, and since the moment of each resultant vector about a point along their line is zero, the following equality holds:

$$\Upsilon\hat{\omega}=0_c \tag{37}$$

Based on Eq. (10), Eq. (37) becomes:

$$[\mathrm{R}_{c,n} \mid {}^*\mathrm{O}_{c,c}](\hat{\omega})=(0_c) \tag{38}$$

Substituting Eq. (33) into (38), Eq. (19) introduced earlier is obtained.

The unknowns in Eq. (19) are the $c$ output angular velocities, and since $c=k-n$ ($c$-circuits, $n$-mobile links, $k$-joints) is the smallest number from the set of characteristics, for any parallel axes EPG mechanism then the following general rule holds:

RULE 2. *In the kinematic analysis of a planar epicyclic mechanism, the use of incidence circuit-joint matrix from an oriented graph and c transfer joints will always lead to a solution with a minimum number of unknowns c.*

In previous work [24,32] it was shown that for a complete kinematic analysis of general planar mechanisms with both revolute and prismatic joints, the minimum number of unknown parameters equals $2c$, where $c$ is the number of independent circuits in the mechanism.

A circuit formulation of the equations of motion, suitable for computer aided analysis, was developed in [33].

## 5 Displacement Analysis for Gear Trains with Parallel Axes of Rotation

**5.1 Absolute Angular Displacements of Gears.** $\theta$ is a $(n\times 1)$ column matrix. Its entries are the absolute angular displacements of all the links of the mechanism (gears and gear carriers) relative to the fixed frame. For matrix $\theta$ the partition is the same as for the absolute angular velocities $\omega$

$$\theta=(\theta_E \mid \theta_c)^T \tag{39}$$

The unknown entries in the column matrix $\theta_c$ are obtained by solving the matrix equation:

$$(\theta_c)=-[{}^0L]^{-1}[L_{c,E}](\theta_E) \tag{40}$$

**5.2 Relative Angular Displacements of Gears $\hat{\boldsymbol{\theta}}$.** The solution for relative angular displacement entries in the $(k\times 1)$ column matrix $\hat{\theta}$ is further obtained as function of absolute angular displacements $\theta$:

$$(\hat{\theta})=\begin{bmatrix} G^T \\ --- \\ {}^*G^T \end{bmatrix}(\theta) \tag{41}$$

For the mechanism in Fig. 1($a$) and in the case of input parameters $\theta_1$ and $\theta_3$ the relative angular positions will be:

$$\begin{aligned}(\theta_{0,1} \quad \theta_{0,2} \quad \theta_{0,3} \quad \theta_{3,4} \mid \theta_{1,4} \quad \theta_{4,2})^T&=(\theta_1 \quad -i_9\, i_{10}\theta_1+(i_9 i_{10}\\ &\quad+1)\theta_3 \;\; \theta_3 \;\; -i_9\theta_1+i_9\theta_3-(i_9+1)\theta_1+(i_9+1)\theta_3(i_9-i_9 i_1 0)\theta_1\\ &\quad+(i_9 i_1 0-i_9)\theta_3)^T\end{aligned} \tag{42}$$

## 6 Acceleration Analysis for Gear Trains With Parallel Axes of Rotation

**6.1 Absolute Angular Acceleration Matrix.** $\varepsilon$ is a $(n\times 1)$ matrix whose entries are the absolute accelerations of all links relative to the fixed frame. If the mechanism has $E$ degrees of freedom, then $E$ values for the absolute accelerations must be assumed known. Following an earlier approach, the partition of matrix $\varepsilon$ will be:

$$\varepsilon=(\varepsilon_E \mid \varepsilon_c)^T \tag{43}$$

For the mechanism Fig. 1($a$) this matrix becomes:

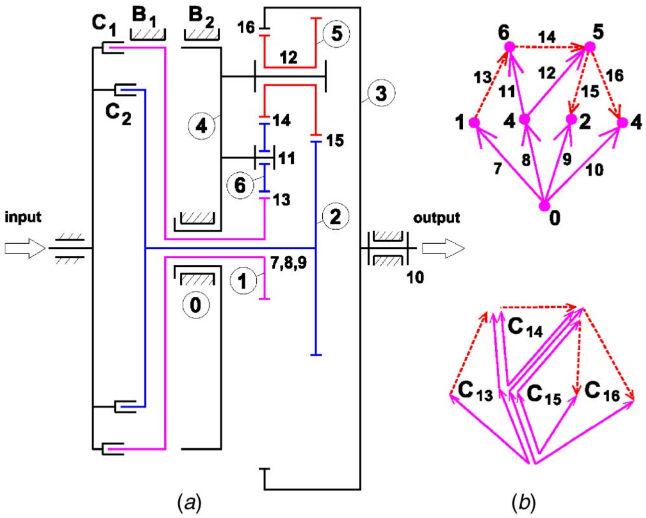


**Fig. 3 Ravigneaux epicyclic transmission: (*a*) mechanism and (*b*) graph and circuits**

$$\varepsilon = (\varepsilon_1 \quad \varepsilon_2 \quad \varepsilon_3 \quad \varepsilon_4)^T \tag{44}$$

In general, for an EGT mechanism with parallel axes of rotation, the matrix equation for accelerations can be written as:

$$\Lambda \varepsilon = 0_c \tag{45}$$

**6.2 Solution of Absolute Angular Acceleration Equations.** The $c$ absolute accelerations required in any dynamic analysis of the mechanism can be easily computed with the following equation:

$$(\varepsilon_c) = -[{}^0L]^{-1}[L_{c,E}](\varepsilon_E) \tag{46}$$

**6.3 Relative Angular Accelerations.** $\hat{\varepsilon}$ Based on the previously calculated absolute accelerations, the relative accelerations between gears or gears and carriers can be further computed with:

$$(\hat{\varepsilon}) = \begin{bmatrix} G^T \\ --- \\ {}^*G^T \end{bmatrix} (\varepsilon) \tag{47}$$

For the mechanism in Fig. 1($a$) with input parameters $\varepsilon_E = (\varepsilon_1 \quad \varepsilon_3)^T$ the relative angular accelerations will therefore be:

$$(\varepsilon_{0,1} \quad \varepsilon_{0,2} \quad \varepsilon_{0,3} \quad \varepsilon_{3,4} \mid \varepsilon_{1,4} \quad \varepsilon_{4,2})^T = (\varepsilon_1 \quad -i_9 i_{10}\varepsilon_1 + (i_9 i_{10} + 1)\varepsilon_3 \quad \varepsilon_3 - i_9\varepsilon_1 + i_9\varepsilon_3 - (i_9+1)\varepsilon_1 + (i_9+1)\varepsilon_3 (i_9 - i_9 i_{10})\varepsilon_1 + (i_9 i_{10} - i_9)\varepsilon_3)^T \tag{48}$$

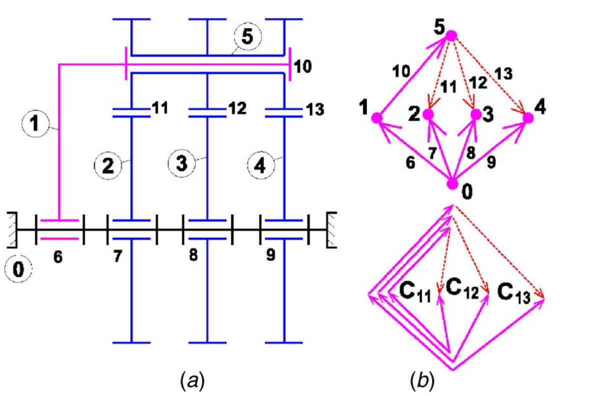


**Fig. 4 Ferguson paradox: (*a*) mechanism and (*b*) graph and circuits**

## 7 Examples

**7.1 Ravigneaux Gear Transmission.** The Ravigneaux EPG mechanism shown in Fig. 3($a$) has $n=6$ mobile links: (1, 2, 3, 4, 5, 6), $k_r=6$ turning joints: (7, 8, 9, 10, 11, 12) and $c=4$ meshing (transfer) joints: (13, 14, 15, 16). The number of degrees of freedom $E=3n-2k_r-c=2$ are the number of inputs in the sequence of activated brakes $B_1$, $B_2$ and clutches $C_1$, $C_2$. The teeth ratios are: $i_{13}=N_1/N_6=d_1/d_6$; $i_{14}=N_6/N_5'=d_6/d_5'$; $i_{15}=N_2/N_5''=d_2/d_5''$; $i_{16}=N_5'/N_3=d_5'/d_3$. In Fig. 3($b$) the graph and in dotted lines the transfer edges (meshing joints), which are removed to obtain the spanning tree, are illustrated.

The reduced incidence matrix and the path matrices of the graph are:

$$[G \mid {}^*G] = \left[\begin{array}{cccccc|cccc} 1 & 0 & 0 & 0 & 0 & 0 & -1 & 0 & 0 & 0 \\ 0 & 0 & 1 & 0 & 0 & 0 & 0 & 0 & -1 & 0 \\ 0 & 0 & 0 & 1 & 0 & 0 & 0 & 0 & 0 & 1 \\ 0 & 1 & 0 & 0 & -1 & -1 & 0 & 0 & 0 & 0 \\ 0 & 0 & 0 & 0 & 0 & 1 & 0 & 1 & 1 & -1 \\ 0 & 0 & 0 & 0 & 1 & 0 & 1 & -1 & 0 & 0 \end{array}\right] \tag{49}$$

$$Z = \begin{bmatrix} -1 & 0 & 0 & 0 & 0 & 0 \\ 0 & 0 & 0 & -1 & -1 & -1 \\ 0 & -1 & 0 & 0 & 0 & 0 \\ 0 & 0 & -1 & 0 & 0 & 0 \\ 0 & 0 & 0 & 0 & 0 & -1 \\ 0 & 0 & 0 & 0 & -1 & 0 \end{bmatrix} \tag{50}$$

while the independent circuit matrix $I$ and the joint position matrix $Y$ are:

$$I = \begin{array}{c} C_{13} \\ C_{14} \\ C_{15} \\ C_{16} \end{array} \left[\begin{array}{cccccc|cccc} 1 & -1 & 0 & 0 & -1 & 0 & 1 & 0 & 0 & 0 \\ 0 & 0 & 0 & 0 & 1 & -1 & 0 & 1 & 0 & 0 \\ 0 & -1 & 1 & 0 & 0 & -1 & 0 & 0 & 1 & 0 \\ 0 & 1 & 0 & -1 & 0 & 1 & 0 & 0 & 0 & 1 \end{array}\right] = [B \mid {}^*U] \tag{51}$$

$$\mathbf{Y} = \left[\begin{array}{cccccc|} \mathbf{y_{13,7}} & -\mathbf{y_{13,8}} & \mathbf{0} & \mathbf{0} & -\mathbf{y_{13,11}} & \\ \mathbf{0} & \mathbf{0} & \mathbf{0} & \mathbf{0} & \mathbf{y_{14,11}} & -\mathbf{y_{14,12}} \\ \mathbf{0} & -\mathbf{y_{15,8}} & \mathbf{y_{15,9}} & \mathbf{0} & \mathbf{0} & -\mathbf{y_{15,12}} \\ \mathbf{0} & \mathbf{y_{16,8}} & \mathbf{0} & -\mathbf{y_{16,10}} & \mathbf{0} & \mathbf{y_{16,12}} \end{array}\right.$$
$$\times \left|\begin{array}{cccc} \mathbf{y_{13,13}} & & & \\ & \mathbf{y_{14,14}} & & \\ & & \mathbf{y_{15,15}} & \\ & & & \mathbf{y_{16,16}} \end{array}\right] = [R \mid {}^*0] \tag{52}$$

Equation (19), for absolute angular velocities:

$$\begin{bmatrix} -i_{13} & 0 & 0 & i_{13}+1 & 0 & -1 \\ 0 & 0 & 0 & i_{14}+1 & -1 & -i_{14} \\ 0 & -i_{15} & 0 & i_{15}+1 & -1 & 0 \\ 0 & 0 & 1 & i_{16}-1 & -i_{16} & 0 \end{bmatrix} \cdot \begin{pmatrix} \omega_1 \\ \vdots \\ \omega_6 \end{pmatrix} = \begin{pmatrix} 0 \\ 0 \\ 0 \\ 0 \end{pmatrix} \tag{53}$$

To the $E=2$ input parameters correspond the following clutch-brake combinations [34]:

*First speed*. Input (clutch $C_{1,}$ and brake $B_2$): $\omega_E = (\omega_1 \ \omega_4)^T = (\omega_1 \ 0)^T$. Output:

$$\omega_c=\begin{pmatrix}\omega_2\\ \omega_3\\ \omega_5\\ \omega_6\end{pmatrix}=\omega_1\begin{pmatrix}-i_{13}i_{14}/i_{15}\\ i_{13}i_{14}i_{16}\\ i_{13}i_{14}\\ -i_{13}\end{pmatrix}$$

*Second speed*. Input (brake $B_1$, and clutch $C_2$): $\omega_E=(\omega_1\ \omega_2)^T=(0\ \omega_2)^T$. Output:

$$\omega_c=\begin{pmatrix}\omega_3\\ \omega_4\\ \omega_5\\ \omega_6\end{pmatrix}=\omega_2\begin{pmatrix}(i_{15}-i_{13}i_{14}i_{15}i_{16})/(i_{13}i_{14}+i_{15})\\ i_{15}/(i_{13}i_{14}+i_{15})\\ (i_{15}-i_{13}i_{14}i_{15})/(i_{13}i_{14}+i_{15})\\ (i_{15}+i_{13}i_{15})/(i_{13}i_{14}+i_{15})\end{pmatrix}$$

*Third Speed*. Input (clutch $C_1$, and clutch $C_2$): $\omega_E=(\omega_1\ \omega_2)^T=(\omega_1\ \omega_1)^T$. Output:

$$\omega_c=\begin{pmatrix}\omega_3 & \omega_4 & \omega_5 & \omega_6\end{pmatrix}^T=\begin{pmatrix}\omega_1 & \omega_1 & \omega_1 & \omega_1\end{pmatrix}^T$$

Equation (53) of absolute angular velocities becomes:

$$\left[\begin{array}{c|cccc}\lambda_1 & 0 & i_{13}+1 & 0 & -1\\ \lambda_2 & 0 & i_{14}+1 & -1 & -i_{14}\\ \lambda_3 & 0 & i_{15}+1 & -1 & 0\\ \lambda_4 & 1 & i_{16}-1 & -i_{16} & 0\end{array}\right]\cdot\begin{pmatrix}1\\ ---\\ \omega_3\\ \vdots\\ \omega_6\end{pmatrix}=\begin{pmatrix}0\\0\\0\\0\end{pmatrix}$$

$$\text{with:}\begin{pmatrix}\lambda_1 & \cdots & \lambda_4\end{pmatrix}=\begin{pmatrix}-i_{13}\omega_1 & 0 & -i_{15}\omega_1 & 0\end{pmatrix}\tag{54}$$

The determinants obtained by removing one column at a time in the Latin matrix:

$$\frac{1}{\Delta_1}=\frac{\omega_3}{-\Delta_3}=\frac{\omega_4}{\Delta_4}=\frac{\omega_5}{-\Delta_5}=\frac{\omega_6}{\Delta_6}$$

have the same value: $-\Delta_3=\Delta_4=-\Delta_5=\Delta_6=i_{13}i_{14}+i_{15}$ and therefore $\omega_3=\omega_4=\omega_5=\omega_6$ which means that links 3, 4, 5 and 6 are rotating as a whole for any input $\omega_E=(\omega_1\ \omega_1)^T$

*Reverse*. Input (clutch $C_2$, and brake $B_2$): $\omega_E=(\omega_2\ \omega_4)^T=(\omega_2\ 0)^T$. Output:

$$\omega_c=\begin{pmatrix}\omega_1\\ \omega_3\\ \omega_5\\ \omega_6\end{pmatrix}=\omega_2\begin{pmatrix}-i_{15}/i_{13}i_{14}\\ -i_{15}i_{16}\\ -i_{15}\\ i_{15}/i_{14}\end{pmatrix}$$

**7.2 Ferguson's Paradox.** Ferguson's mechanism (Fig. 4(*a*)) has $n=5$ mobile links: (1, 2, 3, 4, 5), and has $k=8$ joints, of which $k_r=5$ are turning joints: (6, 7, 8, 9, 10) and $c=3$ are meshing (transfer) joints: (11, 12, 13). The mechanism has two degrees of freedom: $E=3n-2k_r-c=2$. The following velocity inputs are assumed: $\omega_1=10.472$ rad/s, i.e, 100 rpm and $\omega_3=0$, the same as in Ref. [8]. In addition, the following acceleration inputs are considered: $\varepsilon_1=-2.681$ rad/s$^2$, $\varepsilon_3=0$. For the teeth numbers of wheels 2, 3, and 4: $N_2=100$, $N_3=99$, $N_4=101$ and the number of teeth of the compound planet: $N_5'=N_5''=N_5'''=20$, the teeth ratios will be: $i_{11}=N_5'/N_2=20/100$, $i_{12}=N_5''/N_3=20/99$, $i_{13}=N_5'''/N_4=20/101$.

The graph associated to the mechanism is given in Fig. 4(*b*) and the corresponding reduced-incidence and path matrices are:

$$[G\,\vdots\,{}^*G]=\left[\begin{array}{ccccc|ccc}1&0&0&0&-1&0&0&0\\0&1&0&0&0&1&0&0\\0&0&1&0&0&0&1&0\\0&0&0&1&0&0&0&1\\0&0&0&0&1&-1&-1&-1\end{array}\right]\tag{55}$$

$$Z=\begin{bmatrix}-1&0&0&0&-1\\0&-1&0&0&0\\0&0&-1&0&0\\0&0&0&-1&0\\0&0&0&0&-1\end{bmatrix}\tag{56}$$

The independent-circuit matrix $I$, and the joint-positions matrix $Y$ are:

$$I=\begin{array}{c}C_{11}\\C_{12}\\C_{13}\end{array}\left[\begin{array}{ccccc|ccc}1&-1&0&0&1&1&0&0\\1&0&-1&0&1&0&1&0\\1&0&0&-1&1&0&0&1\end{array}\right]=[B\,\vdots\,{}^*U]$$

$$Y=\left[\begin{array}{ccccc|ccc}y_{11,6}&-y_{11,7}&0&0&y_{11,10}&y_{11,11}&0&0\\y_{12,6}&0&-y_{12,8}&0&y_{12,10}&0&y_{12,12}&0\\y_{13,6}&0&0&-y_{13,9}&y_{13,10}&0&0&y_{13,13}\end{array}\right]=[R\,\vdots\,{}^*0]$$

For the input velocities: $\omega_E=(\omega_1\ \ \omega_2)^T=(10.472\ \ 0)^T$, Equation (19) becomes:

$$\left[\begin{array}{cc|ccc}(-i_{11}-1)&1&0&0&i_{11}\\(-i_{12}-1)&0&1&0&i_{12}\\(-i_{13}-1)&0&0&1&i_{13}\end{array}\right]\cdot\begin{pmatrix}\omega_1\\ \omega_2\\ ---\\ \omega_3\\ \omega_4\\ \omega_5\end{pmatrix}=\begin{pmatrix}0\\0\\0\end{pmatrix}\tag{57}$$

and has the solution:

$$\omega_c=\begin{pmatrix}\omega_3\\ \omega_4\\ \omega_5\end{pmatrix}=\omega_1\begin{pmatrix}1-i_{12}/i_{11}\\ 1-i_{13}/i_{11}\\ 1+1/i_{11}\end{pmatrix}=\begin{pmatrix}-0.1058\\ 0.1037\\ 62.8320\end{pmatrix}$$

Equation (57) further becomes:

$$\left[\begin{array}{c|ccc}\lambda_1&0&0&i_{11}\\ \lambda_2&1&0&i_{12}\\ \lambda_3&0&1&i_{13}\end{array}\right]\begin{pmatrix}1\\ ---\\ \omega_3\\ \omega_4\\ \omega_5\end{pmatrix}=\begin{pmatrix}0\\0\\0\end{pmatrix}$$

$$\text{with:}\ \begin{pmatrix}\lambda_1\\ \lambda_2\\ \lambda_3\end{pmatrix}=\begin{pmatrix}-(i_{11}+1)\omega_1+\omega_2\\ -(i_{12}+1)\omega_1\\ -(i_{13}+1)\omega_1\end{pmatrix}\tag{58}$$

The determinants obtained removing one column at a time in the Latin matrix (Eq. (58)) are evaluated to determine potential groups of wheels rotating as a whole:

$$\frac{1}{\Delta_1}=\frac{\omega_3}{-\Delta_3}=\frac{\omega_4}{\Delta_4}=\frac{\omega_5}{-\Delta_5}$$

$$\frac{1}{\begin{vmatrix}0&0&i_{11}\\1&0&i_{12}\\0&1&i_{13}\end{vmatrix}}=\frac{\omega_3}{-\begin{vmatrix}\lambda_1&0&i_{11}\\ \lambda_2&0&i_{12}\\ \lambda_3&1&i_{13}\end{vmatrix}}=\frac{\omega_4}{\begin{vmatrix}\lambda_1&0&i_{11}\\ \lambda_2&1&i_{12}\\ \lambda_3&0&i_{13}\end{vmatrix}}=\frac{\omega_5}{-\begin{vmatrix}\lambda_1&0&0\\ \lambda_2&1&0\\ \lambda_3&0&1\end{vmatrix}}\tag{59}$$

and can be concluded that:

(a) if $i_{12}=i_{13}$ then $-\Delta_3=\Delta_4$, and therefore equal values result for the angular velocities: $\omega_3=\omega_4$ and wheels 3 and 4 are rotating as a whole for any input: $\omega_E=(\omega_1\ \ \omega_2)^T$

(b) if $i_{11}=i_{12}=i_{13}$ and $\omega_2=0$ (wheel 2 fixed) then: $-\Delta_3=\Delta_4=0$, and therefore $\omega_3=\omega_4=0$ (wheel 3 and 4 remain fixed) for any input:$\omega_E=(\omega_1 \quad 0)^T$. For the input angular accelerations: $\varepsilon_E=(\varepsilon_1 \quad \varepsilon_2)^T=(-2.681 \quad 0)^T$, Eq. (45) now becomes:

$$\left[\begin{array}{cc|ccc} (-i_{11}-1) & 1 & 0 & 0 & i_{11} \\ (-i_{12}-1) & 0 & 1 & 0 & i_{12} \\ (-i_{13}-1) & 0 & 0 & 1 & i_{13} \end{array}\right] \cdot \begin{pmatrix} \varepsilon_1 \\ \varepsilon_2 \\ \hline \varepsilon_3 \\ \varepsilon_4 \\ \varepsilon_5 \end{pmatrix} = \begin{pmatrix} 0 \\ 0 \\ 0 \end{pmatrix} \tag{60}$$

and the solution (46) yields:

$$\varepsilon_c = \begin{pmatrix} \varepsilon_3 \\ \varepsilon_4 \\ \varepsilon_5 \end{pmatrix} = \varepsilon_1 \begin{pmatrix} 1 - i_{12}/i_{11} \\ 1 - i_{13}/i_{11} \\ 1 + 1/i_{11} \end{pmatrix} = \begin{pmatrix} 0.0271 \\ -0.0265 \\ -16.0860 \end{pmatrix} \tag{61}$$

This is called Ferguson's paradox because $\omega_3$ and $\omega_4$ are of close values but have opposite signs, and have a high reduction ratio relative to the driving carrier 1.

## 8 Conclusions

A novel technique for angular positions, velocities, and accelerations analysis of parallel-axes epicyclic gear trains has been presented. The method is based on the transfer-joint, link-joint and circuit-joint incidence matrix of the oriented graph associated with the mechanism. Based on a set of circuits (which is the base of a cycle matroid derived from the oriented graph attached to the mechanism), the independent set of kinematic equations in a minimum number of variables can be generated. Following the proposed approach, the Latin matrix, having its entries as functions of speed ratios, can then be automatically calculated. Any possible singularity of the mechanism can then be determined in a systematic way by checking the rank of this Latin matrix. Using the same base of circuits of the cycle matroid, an independent set of matrix equations for acceleration analysis can be generated easily and quickly.

The proposed technique is very well suited to computer implementation and allows an automatic generation of the kinematic equations of any epicyclic transmission with any number of gears and degrees of freedom.

## References


[1] Willis, R., 1870, *Principles of Mechanism*, 2nd Ed., Longmans, Green and Co., London.

[2] Ravigneaux, P., 1930, "Theorie Nouvelle sur les Trains Epicycloidaus et les Mouvements Relatifs," La Technique Automobile et Aerienne, 21, pp. 97–106.

[3] Voinea, R., and Atanasiu, M., 1964, *New Analytical Methods in Mechanism Theory*, Editura Tehnica, Bucharest (in Romanian).

[4] Glover, J. H., 1965, "Efficiency and Speed-Ratio Formulas for Planetary Gear Systems," Prod. Eng. (N.Y.), **27**, pp. 72–79.

[5] Levai, Z., 1968, "Structure and Analysis of Epicyclic Gear Trains," J. Mech., **3**, pp. 131–148.

[6] Martin, G. H., 1969, *Kinematics and Dynamics of Machines*, McGraw-Hill, New York, pp. 298–306.

[7] Cleghorn, W. L., and Tyc, G., 1987, "Kinematic Analysis of Planetary Gear Trains Using a Microcomputer," Int. J. Mech. Eng. Educ., **15**, pp. 57–69.

[8] Norton, R. L., 2004, *Design of Machinery*, McGraw-Hill, New York, pp. 497–499.

[9] Buchsbaum, F., and Freudenstein, F., 1970, "Synthesis of Kinematic Structure of Geared Kinematic Chains and Other Mechanisms," J. Mech., **5**, pp. 357–392.

[10] Freudenstein, F., 1971, "An Application of Boolean Algebra to the Motion of Epicyclic Drives," Veh. Syst. Dyn., **93**, pp. 176–182.

[11] Hsu, C. H., and Lam, K. T., 1992, "A New Graph Representation for the Automatic Kinematic Analysis of Planetary Spur-Gear Trains," ASME J. Mech. Des., **114**, pp. 196–200.

[12] Tsai, L. W., 1988, "The Kinematics of Spatial Robotic Bevel-Gear Trains," Rob. Comput.-Integr. Manufact., **4**, pp. 150–155.

[13] Chatterjee, G., and Tsai, L. W., 1996, "Computer-Aided Sketching of Epicyclic-Type Automatic Transmission Gear Trains," ASME J. Mech. Des., **118**(3), pp. 405–411.

[14] Shai, O., and Pennock, G. R., 2006, "Extension of Graph Theory to the Duality Between Static Systems and Mechanisms," ASME J. Mech. Des., **128**(1), pp. 179–191.

[15] Nelson, C. A., and Cipra, R. J., 2005, "Simplified Kinematic Analysis of Bevel Epicyclic Gear Trains With Application to Power-Flow and Efficiency Analyses," ASME J. Mech. Des., **127**, pp. 278–286.

[16] Gudal, S., Pan, Y., Liou, S. Y., Sundararajan, V., Antonetti, D., and Wright, P. W., 2004, "Design System for Composite Transmission Error Prediction for Automatic Transmission," 2004 ASME DETC, Paper no. DETC2004-57721.

[17] Shai, O., and Preiss, K., 1999, "Graph Theory Representation of Engineering Systems and their Embedded Knowledge," IEEE Trans. Control Syst. Technol., **13**(2), pp. 273–284.

[18] Dunn, A. L., Houser, D. R., and Lim, T. C., 1999, "Methods for Researching Gear Whine in Automotive Transaxles, " J. Passen. Cars: Mech. Syst., 118(6), pp. 2849–2858.

[19] Kahraman, A., 1994, "Planetary Gear Train Dynamics," ASME J. Mech. Des., **116**, pp. 713–720.

[20] Talpasanu, I., 1991, "Optimization of the Kinematic Calculation of the Plane and Spatial Solid Body Systems," International Association for Advancement of Modelling and Simulation Techniques in Enterprises (AMSE) Conference, New Orleans, LA, October 28-30, pp. 99–109.

[21] Recski, A., 1989, *Matroid Theory and its Applications in Electric Network Theory and in Statics*, Springer, Berlin.

[22] Kavesh, A., 1997, *Optimal Structural Analysis*, Research Studies Press (Wiley), Exeter, U.K.

[23] Shai, O., 2001, "The Multidisciplinary Combinatorial Approach and its Applications in Engineering," Artif. Intell. Eng. Des. Anal. Manuf., **15**, pp. 109–144.

[24] Talpasanu, I., 2004, "Kinematics and Dynamics of Mechanical Systems Based on Graph-Matroid Theory," Ph.D. Dissertation, University of Texas at Arlington.

[25] Oxley, J., 1992, *Matroid Theory*, Oxford University Press Oxford.

[26] Zhou, H., and Ting, K. L., 2005, "Topological Synthesis of Compliant Mechanisms Using Spanning Tree Theory," ASME J. Mech. Des., **127**, pp. 753–759.

[27] Whitney, H., 1935, "On the Abstract Properties of Linear Dependence," Am. J. Math., **57**, pp. 509–533.

[28] White, N., ed., 1986, *Theory of Matroids*, Cambridge University Press, Cambridge.

[29] Kutzbach, K., 1929, "Mechanische Leitungverzweigung; ihre Gasetze und Anwendungen," Machinenbau, der Betrieb, **8**, pp. 710–716.

[30] Hsieh, H. I., and Tsai, L. W., 1996, "Kinematic Analysis of Epicylic-Type Transmissions Mechanisms Using the Concept of Fundamental Kinematic Entities," ASME J. Mech. Des., **118**(2), pp. 294–299.

[31] Selgado, D. R., and Del Castillo, J. M., 2005, "A Method for Detecting Degenerate Structures in Planetary Gear Trains," Mech. Mach. Theory, **40**, pp. 948–962.

[32] Voinea, R., Atanasiu, M., Iordache, M., and Talpasanu, I., 1983, "Determination of the Kinematic Parameters for a Planar Linkage Mechanism by the Independent Loop Method," Proceedings of the Fifth International Conference on Control Systems and Computer Science, Bucharest, 1, pp. 20–23.

[33] Lang, S. Y.T., 2005 "Graph-theoretic modeling of epicyclic gear systems," Mech. Mach. Theory, **40**, pp. 511–529.

[34] Simionescu, P. A., Beale, D. G., and Dozier, G. V., 2006, "Teeth-Number Synthesis of a Multispeed Planetary Transmission Using an Estimation of Distribution Algorithm," ASME J. Mech. Des., **128**, pp. 108–115.